Distributed spectral measurement of nonlinear Raman cascade process along an optical nanofiber

Yosri Haddad, Jean-Charles Beugnot, Samuel Margueron, Gil Fanjoux

Distributed spectral measurement of nonlinear Raman cascade process along an optical nanofiber

Yosri Haddad, Jean-Charles Beugnot, Samuel Margueron and Gil Fanjoux*
FEMTO-ST Institute, UMR 6174 CNRS / Université Bourgogne Franche-Comté, 15B avenue des Montboucons, 25030 Besançon - France

ABSTRACT

We present in this work the longitudinal characterization of the spectral evolution of a Raman cascading process along an optical nanofiber with a millimetric length and sub-micrometric size. The measurements are performed by analyzing with a confocal micro-spectrometer the light radiated by Rayleigh scattering out the nanofiber. This observation is performed with a high spatial resolution given by a confocal microscope, and a high spectral resolution given by the spectrometer.

Keywords: Raman cascade process, Rayleigh scattering, optical nanofiber, spectrometer.

1. INTRODUCTION

Simultaneous spatial and spectral measurements of the longitudinal evolution of the guided light all along an optical waveguide operating in the nominal regime is of great interest in the field of optical metrology. Indeed, this information is first useful to validate or improve the numerical and theoretical predictions. In addition, this information is crucial for waveguide engineering because of the direct access of the local losses, defects and modal behavior for example. Specifically in nonlinear regime, their operation under such conditions, as well as their fabrication methods, induce complex losses and nonlinear behaviors that remain difficult to understand and to integrate in a complete approach. Therefore, an experimental investigation of distributed measurements along waveguides is crucial for the development of micro- and nano- photonics waveguides. Conjugated spectral and spatial resolutions would allow the analysis of the evolution of spectral components generated along waveguides by nonlinear effects such as stimulated Raman scattering, four wave mixing, second harmonic generation, etc. These distributed measurements will complement the current characterization methods of optical waveguides focused either on the output or input side of the waveguide in order to analyze the transmitted or backscattered field in power, polarization, or spectrally. They will also complement other distributed measurement along the waveguide based on reflectometry or cutback techniques for example, which provide, however, non-spectrally resolved measurements or destructive method.

In this context, a spectroscopic technique is developed in this work in order to characterize spatially and spectrally the evolution of the guided light along an optical waveguide in nominal operation. This experimental technique is based on the detection of the right-angle radiated field by Rayleigh scattering (RS) process outside the waveguide by using a confocal micro-spectrometer. This system allows the observation of the longitudinal evolution of the radiated field along the waveguide optical axis. The method presents the advantage of being non-destructive, non-invasive, and to present simultaneously a micrometric spatial resolution and a high spectral resolution. Moreover, this technique can be used in linear and nonlinear regime, with continuous or pulsed laser sources, at different pump laser wavelengths, and with different geometry of waveguides.

To confirm the large flexibility of our experimental technique, the present work concerns the spectral characterization of a Raman cascading process along a sub-micrometric diameter tapered fiber (called nanofiber thereafter), homogeneous along several centimeters, and pumped in the visible wavelength range and in the sub-nanosecond regime. Optical nanofiber (ONF) present a large interest in a wide number of applications due to their specific properties, i.e., the high intensity of the confined field, and a strong evanescent field in interaction with the surrounding medium. Then, applications in both linear and nonlinear regimes go from atom trapping in the evanescent field [1,2] to supercontinuum generation [3,4], efficient evanescent Raman scattering [5], evanescent Kerr effect [6] and provides advances in quantum information technologies [7,8]. Therefore, optical characterization along an ONF is highly useful for different input power and wavelength, which is not possible by any current characterization systems. The generation of the Raman cascading process in ONF is clearly visible with an exponential increase of the Stokes and anti-Stokes spectral components as excepted. Furthermore, the longitudinal evolution of the intensities of the first three Raman Stokes orders is in good agreement with

*gil.fanjoux@univ-fcomte.fr; phone +33 3 81 66 64 26; https://www.femto-st.fr/

the theory, showing that our technique can provide quantitative data without any numerical post-processing. It is noteworthy that this method can be extended to others waveguides whatever its geometry which represents a strong interest for deepen optical characterization of photonics waveguides, or for other optical regimes characterized by spectral evolution of the field propagating along an optical waveguide in nominal operation.

2. EXPERIMENTAL SETUP

The experimental setup is illustrated in Fig. 1(a). It consists of a confocal Raman micro-spectrometer (Monovista, S-&-I GmbH) centered on the Rayleigh scattering (RS) detection (obtained by removing the Notch filter of the spectrometer). The system is equipped with a high-precision motorized stage for longitudinal X and transverse Y displacement of the waveguide under study and a microscope objective translation Z, all with a step size and reproducibility better than <100 nm. This system allows the generation of an accurate recordable 3D spatial trajectory point-by-point all along the waveguide under test. Therefore, after having recorded the trajectory corresponding to the waveguide, the system allows us to measure a $1D{-}X$ RS trace along the X waveguide axis or $1D{-}Y{-}Z$ RS trace perpendicular to the waveguide, or a $2D{-}XY{-}XZ{-}YZ$ maps in the XY or XZ planes containing the waveguide or in the YZ plane perpendicular to the waveguide. The RS of the guided light in the optical waveguide medium, which exits to the outside, is collected in the Z right angle to the propagation direction X (Fig. 1(a)) with a x10 microscope objective and recorded through the spectrometer. The monochromator is equipped with three diffraction gratings (300, 1500 and 2400 lines/mm), and a back-illuminated cooled CCD detector (-85 C°) leading to a low detection threshold and a high signal-to-noise ratio (SNR). Alternatively, an imaging system composed of a CCD camera can image the waveguide for positioning the waveguide at the optical axis of the RS detection system, and also for rough fiber diameter measurements.

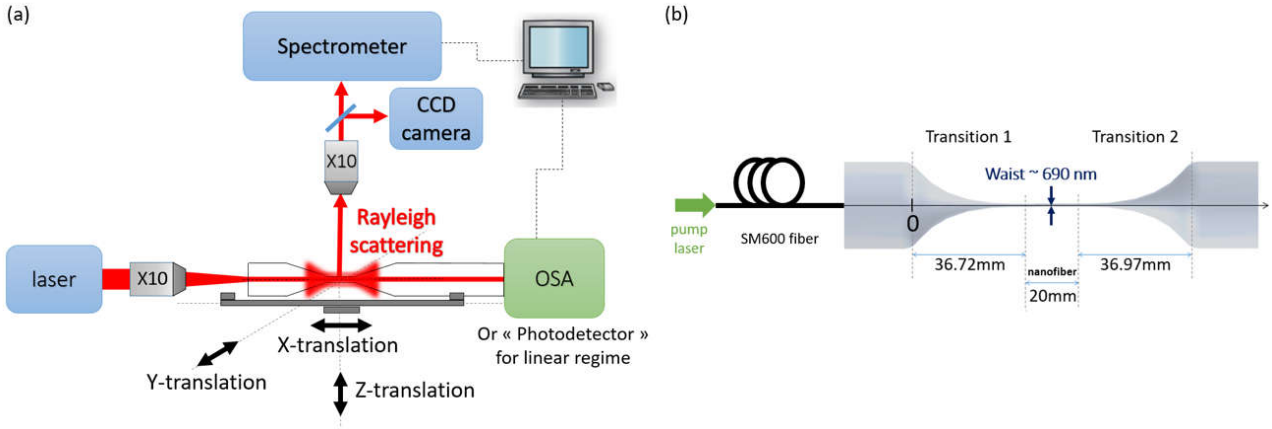

Figure 1. Experimental setup: (a) Schematic experimental setup (b) geometrical data of the ONF.

Even if the method can be used for any type of optical waveguide, this work focuses on ONF. Note that ONF study in this work represents a challenge because this waveguide is not perfectly straight and the 3D trajectory have to be done accurately to follow very precisely the transitions and ONF regions. The ONF studied in our work corresponds to a standard single-mode fiber at telecom wavelength (SMF-G652D) obtained by the heat-and-pull method [9,10] up to obtain a fiber portion with a diameter of 690 nm accurately measured by Brillouin scattering method and homogeneous up to two centimeters in length [11]. The optical losses were measured just after manufacturing between −1.5 and −4 dB at 532 nm of wavelength, strongly depending on the injection of the laser beam in this multi-mode fiber. Therefore, this high level of losses is certainly due to the modal filtering by the taper part of the waveguide, which is not adiabatic for the all injected modes. Just after manufacturing, the ONF is placed inside closed transparent plexiglass boxes in order to protect it from external air vibrations and to reduce any kind of contamination by dust for example [12].

Measurements were performed following two steps. First, we have evaluated the 3D-XYZ spatial trajectory of the whole taper in the linear regime in order to precisely locate the position of the ONF in the taper fiber. Then we have investigated the longitudinal evolution of the Raman cascade process in the nonlinear regime. For the linear regime, we use a power stabilized *cw* laser diode with a wavelength of 653 nm. The input laser power is typically between 2 and 3 mW in order to limit the thermal effects or to avoid the ONF breaking. The laser power is simultaneously monitored in the transmitted power during the measurements (see Fig.1(a)) without significant variation of the output power. The 3D- XYZ spatial

trajectory, which follows the waveguide, is made in two steps. We first roughly locate the optical taper with the CCD imaging system for the X, Y and Z coordinates, and thereafter we optimize the scattering signal for each position by adjusting precisely the Y and Z positions with the minimal entrance slit width in order to have the highest spatial resolution, typically 5 µm. Then, we record several positions (X,Y,Z), point by point, along the waveguide with a step size of about 10 mm. The second step corresponds to the interpolation between these points in order to obtain a trajectory with the desired number of points. Furthermore, the exposure time is in general case equal to about 0.5 s per point. Once we identify the exact position of the ONF part of the tapered fiber, we pump the fiber with the pulsed laser source in order to investigate the longitudinal spectral evolution of the light mode in the nonlinear regime of propagation. For that purpose, the fiber is pumped by a laser source corresponds to a doubled-frequency microchip Nd:YAG laser, with a repetition rate of 21 kHz and 500 ps of pulse duration. The laser beam is first injected in a small core fiber (SM600), connected to the tapered fiber. This system allows the control of the injection in the SMF fiber core preferentially in the fundamental mode of the non-stretched part of the fiber taper. The spectrum at the fiber output is measured by an OSA (optical spectrum analyzer) every 7 seconds simultaneously with the Rayleigh scattered signal measurements in order to be sure that the Raman cascading process is stable during all the 1D-scan-X over a duration of approximately one hour. Concerning the Raman spectrometer, three Notch filters were used in order to only remove the pump Rayleigh component. The entrance slit was equal to 1 mm, and 50 points were performed, i.e., one point every 400 μm.

In terms of data acquisition and treatment, the RS data were recorded in the same experimental conditions. It is noteworthy that no normalization or correction of intensity point by point has been applied for the different 1D-X scans and the raw data are directly given in this paper.

3. EXPERIMENTAL RESULTS

1.1 Linear regime

Figure 2(a) shows the 1D-X scattering trace obtained for the tapered fiber with the *cw* laser source at $\lambda = 653$ nm of wavelength with our technique (red curve), and compared to the trace obtained with an optical backscattered reflectometer (OBR) working at $\lambda = 1566\ nm$ for the same fiber (OBR4600 form Luna – blue curve). The fiber is thus in single-mode regime for the OBR trace and multi-mode regime for the RS trace. The scattering profiles are similar with a general point of view, which proves that our system is relevant. These scattering profiles are indeed due to the characteristics of the different scattering sources, corresponding to the fiber core at the beginning of the transition where light is still guided into the core of the fiber, the silica cladding when the core is no longer guiding in the tapered region, and the ONF surface for the small diameter when the surface scattering takes over the cladding scattering [13,14].

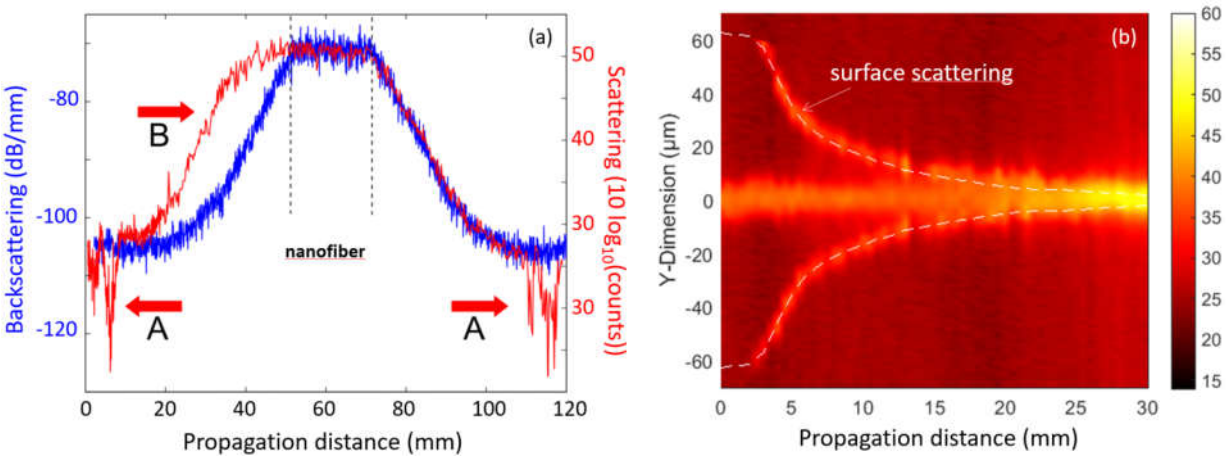

Figure 2. (a) 1D-X Rayleigh scattering trace obtained fiber with the *cw* laser source at a wavelength of $\lambda = 653$ nm (red curve) and OBR trace obtained at $\lambda = 1566\ nm$ (blue curve). The black arrows: (A) show two successive decreases of the scattering level at the level of the transition 1 and 2, and (B) shows the blurred scattering level along the first transition region due to the filtering process by the transition of the lossed modes. Blue curve corresponds to a symmetrical scattering profile and is only intended to show a trend. (b) 2D scan for the input transition of the fiber. White dashed line corresponds to the fiber shape.

As the ONF has a homogenous diameter along about 20 mm length, the scattering level remains constant as observed in the 1D-X trace. The two successive decreases of the scattering level at the beginning of the transition 1 and at the end of the transition 2 (arrow A), originate, respectively, from the expansion of different optical modes from the fiber core region into the cladding region, and from the back coupling of these modes from the cladding region into the core at the same fiber diameters at the level of the transition 2. These two characteristics are not visible in the OBR trace (blue curve) because the fiber is injected preferentially in the fundamental mode and therefore the fiber is single-mode. On the other hand, for low diameters in the transition 1, the RS signal shows a large increase of the scattering level (arrow B), contrary to the RS signal in transition 2, and contrary to the OBR trace. This scattering feature should come from the scattering of different radiation modes, which are no more supported by the transition 1 when reaching the cut-off diameter. To confirm that assumption, Fig. 2(b) represents a 2D map of the scattered intensity along the transition 1, which highlights the scattering from the surface of the fiber along the input transition level. We clearly observe the scattering process at the surface of the transition 1 by the radiation HOMs, which are no more guided by the clad of the fiber. This means that the transition is not adiabatic for all the optical modes initially propagating inside the core region of the unstretched part of the SMF-G652D fiber. The fact that this scattering in not visible in transition 2 confirms this observation.

Therefore, from this 1D-X trace in the linear regime (Fig.2(a)), it is clear that the ONF region is exactly located between, X = 50 mm and X = 70 mm. Now, by using this information, we will present in the following paragrapth the results obtained for the Raman cascading process evolution along this targeted region of the tapered fiber in the nonlinear regime by using the sub-picosecond laser source.

1.2 Nonlinear regime: Raman cascading process along the nanofiber

In the nonlinear regime of the light propagation, all the difficulty corresponds to the detection of a weak scattering signal. Indeed, the system have to detect the Raman spectral components, which have lower intensities than the pump source, scattered by the Rayleigh scattering process originated from the refractive index fluctuations within the fiber. Second, as the laser source is pulsed in order to reach the nonlinear regime of the light propagation, the number of scattered photons decreases once again as opposed to the linear regime where the light source is a *cw* source and the scattering level is high. Therefore, the intensity of the scattered signal outside the fiber is extremely weak in this case. However, to overcome these limitations, the detection was made possible by the low level of detection of the cooled CCD detector of the spectrometer, and by a long exposure time of the spectrometer detector, typically 60 s per point. In addition, the large width of the entrance slit of the spectrometer (1 mm) used for this measurements increases the number of the detected Rayleigh photons. Moreover, the 1D-scan-X has been performed only for the ONF part (between X=50-70 mm), i.e., with the homogeneous diameter, where the strength of the scattering process is maximal and constant due to the large difference in the refractive index of air and dielectric [13]. This ensures a scattered recorded signal with a high intensity and a stable SNR in order to observe the real dynamics of the Raman amplifications of the all generated spectral components along the ONF region.

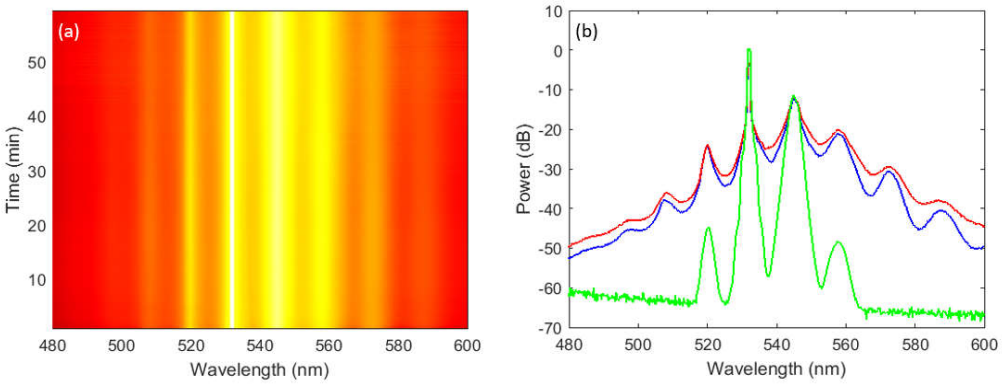

Figure 3. (a) Evolution of the spectrum at the output of the fiber recorded by an OSA. (b) The first (blue curve) and the last (red curve) OSA spectrum. The green spectrum corresponds to the spectrum at the output of the SM600 fiber.

Figure 3(a) shows the evolution of the output spectrum of the whole fiber recorded by an optical spectrum analyzer (OSA). The spectrum is clearly stable over one hour without significant variations. Figure 3(b) shows that the first (blue curve) and the last (red curve) spectrum are almost similar. In addition, the spectrum in dashed green curve represents the spectrum at the output of the SM600 fiber. As the core diameter of the standard fiber SMF-G652D is greater than for the SM600,

then the field spectrum should not strongly evolve up to the beginning of the first transition of the ONF, because of the lower intensity than in the SM600 fiber.

Figure 4(a) shows the evolution of the spectrum along the homogeneous part of the ONF region. It is the first time, to our knowledge, that the spectral longitudinal evolution in nonlinear regime along a ONF is observed. The Raman cascading process is clearly visible with the generation of several Raman Stokes and anti-Stokes orders. Even if the ONF length is short (about 2 cm), the Raman amplification is efficient due to the large reduction of the effective area of the guided modes which provides a strong confinement of the light modes in the ONF. Hence, this leads to increase the light-matter interactions, giving rise to high-efficiency nonlinear frequency conversions of the different Raman Stokes and anti-Stokes components. Furthermore, Fig. 4(b) compares the first and the last spectrum, and shows the dynamics of the measurement (about 40 dB) allowing the clear observation of the spectral evolution.

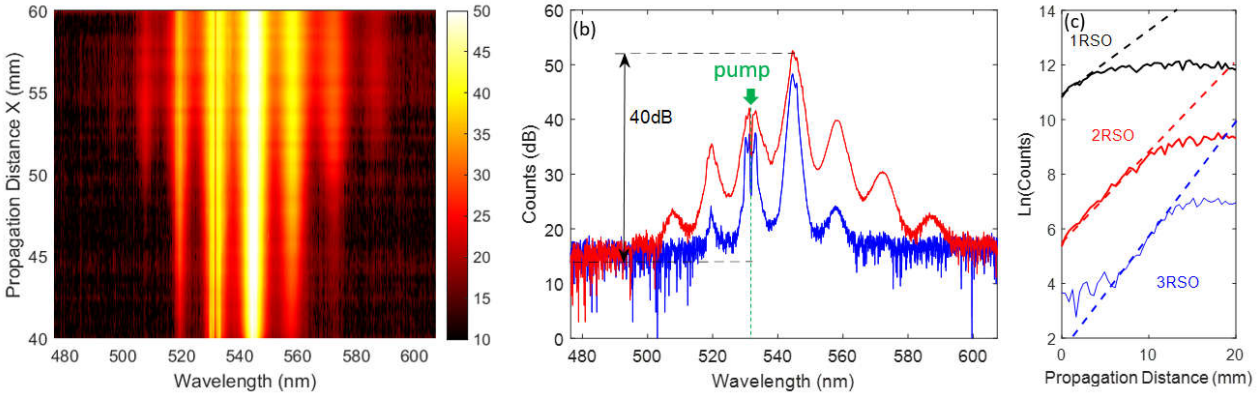

Figure 4. (a) Evolution of the scattered Raman cascade spectrum along the ONF region. (b) The input (blue curve) and the output (red curve) spectrum for the ONF. (c) Evolution of the natural logarithm of peaks of the different spectral components in the Stokes region with the propagation distance X. The dashed lines have been used to estimate slopes.

Figure 4(c) represents the evolution of the natural logarithm of the different spectral Stokes components peaks along the ONF distance X. The exponential Raman amplification, characterized by a linear evolution, is clearly visible for all the Raman Stokes orders, from their generation up to the depletion of their respective pump. Assuming that the detector response is almost flat for the spectral range concerned between the pump and the 3rd order Raman Stokes (532 nm up to 573 nm), the linear slope of the intensity evolution for the first, second and third Raman Stokes orders can be roughly estimated. The first Raman Stokes order presents a slope of about 0.18 mm^{-1}, 0.35 mm^{-1} for the second Raman Stokes order, and 0.53 mm^{-1} for the third Raman Stokes order. The theory predicts that the slope is multiplied by a factor of two between the first and the second Raman Stokes order, and by a factor of three between the first and the third Raman Stokes orders. The experimental measurements thus show that the evolution of the spectra are in good quantitative agreement with the theory [15].

4. CONCLUSION

The experimental results prove that the experimental technique based on right-angle Rayleigh scattering measurements is a powerful tool to characterize the conjugated spatial and spectral evolution of the field propagating along a photonic waveguide. In linear regime, this technique allows the identification of optical losses, mode behavior along a variable diameter fiber, mode beating and local defects with high reproducibility. In nonlinear regime, we have observed for the first time to our knowledge the Raman cascading process all along an optical nanofiber with quantitative evolution of the different spectral components generated during the propagation.

The perspective of the technique are numerous. The technique could be extended to study other waveguides with complex geometry such as ridge, spiral, or optofluidic guides for instance. The intensity and spatial sensitivity of Rayleigh scattering can also be used to detect local scattering process induced in a Bragg grating fiber, local doping or local temperature evolution. Additionally, other nonlinear processes along a waveguide such as second harmonic generation along ridge waveguides, generation of the hyper-Rayleigh scattering process, or the development of the Raman scattering process into a supercontinuum generation along nonlinear waveguides can be studied.

ACKNOWLEDGMENT

This work has been supported by the EIPHI Graduate School (contract ANR-17-EURE-0002) and by the Conseil Régional de Bourgogne - Franche-Comté (DECAP and CIPPIC project).
Authors thank Thibaut Sylvestre for relevant and helpful discussions.

REFERENCES

[1] Le Kien, F., Gupta, S. D., Balykin, V., and Hakuta, K., "Spontaneous emission of a cesium atom near a nanofiber: Efficient coupling of light to guided modes," Phys. Rev. A 72(3), 032509 (2005).
[2] Morrissey, M. J., Deasy K., Frawley M., Kumar R., Prel, E., Russell, L., Truong, V. G., and Nic Chormaic, S., "Spectroscopy, manipulation and trapping of neutral atoms, molecules, and other particles using optical nanofibers: a review, " Sensors 13(8), 10449–10481 (2013).
[3] Birks, T., Wadsworth, W., and Russell, P. S. J., "Supercontinuum generation in tapered fibers," Opt. Lett. 25(19), 1415–1417 (2000).
[4] Ying, P., Feng, G., Li, X., Ma, Z., Chen, J. Zhu, Q., and Zhang, X., "Supercontinuum generation based on nanofiber," Optik 119(13), 648–653 (2008).
[5] Shan, L. Pauliat, G., Vienne, G., Tong, L., and Lebrun, S., "Stimulated raman scattering in the evanescent field of liquid immersed tapered nanofibers," Appl. Phys. Lett. 102(20), 201110 (2013).
[6] Fanjoux, G., Chrétien, J., Godet, A., Phan-Huy, K., Beugnot, J.-C., and Sylvestre, T., "Demonstration of the evanescent kerr effect in optical nanofibers,"Opt. Express 27(20), 29460–29470 (2019).
[7] O'Shea, D., Junge, C., Volz, J., and Rauschenbeutel, A., "Fiber-optical switch controlled by a single atom," Phys. Rev. Lett. 111(19), 193601 (2013).
[8] Petersen, J., Volz, J., and Rauschenbeutel, A., "Chiral nanophotonic waveguide interface based on spin-orbit interaction of light," Science 346(6205), 67–71 (2014).
[9] Tong, L and Sumetsky, M., "Subwavelength and nanometer diameter optical fibers," Springer Science & Business Media," (2011).
[10] Tong, L., Gattass, R. R., Ashcom J. B., He, S., Lou, J., Shen, M., Maxwell, I., and E. Mazur, "Subwavelength-diameter silica wires for low-loss optical wave guiding," Nature. 426(6968), 816–819 (2003).
[11] Godet. A, Ndao, A., Sylvestre, T., Pecheur, V., Lebrun, S., Pauliat, G., Beugnot, J.-C., and Huy, K. P., "Brillouin spectroscopy of optical microfibers and nanofibers," Optica. 4(10), 1232–1238 (2017).
[12] Fujiwara M., Toubaru, K., and Takeuchi, S., "Optical transmittance degradation in tapered fibers," Opt. Express 19(9), 8596–8601 (2011).
[13] Haddad, Y., Chrétien, J., Beugnot, J. C., Godet, A., Phan-Huy, K., Margueron, S., & Fanjoux, G., "Microscopic imaging along tapered optical fibers by right-angle Rayleigh light scattering in linear and nonlinear regime," Optics Express, 29(24), 39159-39172 (2021).
[14] Lai, Y.-H., Yang, K. Y., Suh, M.-G., and Vahala, K. J., "Fiber taper characterization by optical backscattering reflectometry," Opt. Express 25(19), 22312–22327 (2017).
[15] Boyd, R. W., "Nonlinear Optics," Academic press" (2020).